



Temperature stratification in the Sun's photosphere in high horizontal resolution using Ca II H filtergrams

V. M. J. Henriques^{1,2} and D. Kiselman¹

¹ Institute for Solar Physics, Royal Swedish Academy of Sciences, AlbaNova University Center, SE-106 91 Stockholm, Sweden

² Stockholm Observatory, Stockholm University, Sweden e-mail: vasco@astro.su.se

Abstract. A method to extract the temperature stratification in the Sun's photosphere using filtergrams is presented along with some high resolution results. The data was acquired with the Swedish 1-m Solar Telescope (SST) using a tunable filter in the Ca II H blue wing. Each full scan is completed in the order of seconds thus allowing for the full resolution of the SST and reasonable depth sampling to be obtained simultaneously in a shorter time than that of the evolution time scale of the photosphere. We test the quality of the method by applying it to a set of synthetic images (obtained through radiative transfer on 3D HD and MHD simulation snapshots followed by degradation) and comparing the output with the known 3D simulated atmosphere. Fine structure around bright points becomes evident in both the temperature gradient maps computed from a set of test observations and synthetic images obtained from MHD simulations.

Key words. Sun: High Resolution – Sun: Temperature Stratification

1. Introduction

The photospheric temperature stratification can be obtained in a fairly straightforward way from the wide Ca II H and K wings following Shine & Linsky (1974) formulation which assumes LTE and hydrostatic equilibrium. At the SST we are exploiting this diagnostic in high horizontal resolution via a simple setup consisting of a 1 Å Ca II H core filter assembled in a rotation stage. With increasing tilt angle the central wavelength of the filter's transmission will shift to the blue thus providing a way to scan the blue wing (Fig. 1). This provides filtergrams that can potentially reach the diffraction limit of 0.1'' resolution.

Furthermore, the use of filtergrams allows for a very high cadence with each full scan (and thus each full 3D map) taking a typical time of 10 seconds, which is of the order of the evolution time scale of the photosphere at this resolution. Since this setup is assembled in parallel with the CRISP Imaging Spectropolarimeter, the high resolution temperature stratification obtained with Ca II H can then be used, for example, to improve full Stokes inversions using lines such as 6302. However, the simple setup consisting of a tiltable interference filter will lead to broadened filter profiles, an elongated PSF from apodization effects and the inclusion of many line blends into the observed image. Apodization effects are minimized by applying

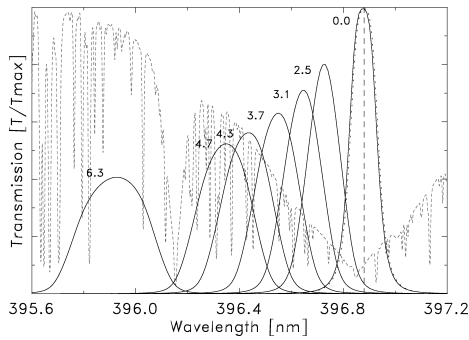


Fig. 1. The different transmission profiles of the interference filter for different tilt angles.

a combination of MOMFBD (van Noort et al. 2005) and deconvolution with the known elongated PSF as described in Löfdahl & Scharmer (2004). Blends are corrected for at the time of intensity calibration by using a synthetic Ca II H profile with no blends computed from a reference atmosphere (at the moment we use the Holweger & Mueller 1974, atmosphere) known to reproduce the average quiet sun spectra. To quantify the quality of the end result, synthetic images computed from known 3D atmospheres and degraded first to an ideal level and later to match the quality of one set of observations, were used.

2. Testing

3D atmosphere simulation snapshots computed with the Stein & Nordlund (1998) code and kindly provided by Mats Carlsson were used to generate the synthetic images. These include both HD and MHD simulations. We used MULTI (Carlsson 1986) for the radiative transfer. For every horizontal point of the simulation, MULTI was run as in a 1D atmosphere in NLTE using 3 rays. While the inversion technique assumes LTE, we want any NLTE effect to show up in the tests. All possible blends were included as background opacities from the VALD database (Ryabchikova et al. 1999; Piskunov et al. 1995). Synthetic images for each tilt angle were then generated by applying the shifted filter profiles. Degradation on these synthetics was first applied using the

telescope’s ideal PSF. Then our code was applied to these synthetic observations and compared with the known 3D atmosphere column by column. Statistics of the errors can be seen in Table 1 where we have averaged the statistics over the 6 filter positions in order to fit in this short paper.

To quantify the quality of the inversions in specific observations, we also devised a non-ideal degradation scheme based on the assumption that continuum synthetic images degraded with the telescope’s real PSF should match the power spectra of the observed continuum images. This assumption is indirectly supported by the match obtained between the intensity histograms of synthetics and observations using Hinode’s non-ideal PSF in Wedemeyer-Böhm & Rouppe van der Voort (2009). The temperature extraction code is then also applied to the synthetics degraded in this way. The results are shown in Table 1 under “full degradation” and provide a measure for how accurate the temperature inversions from the sample observations shown in this paper are. The selection of HD for the known atmosphere in the table was due to the fact that very few magnetic elements were present in the observations and the maximum filter tilt is not close enough to the continuum for the RMS of an HD synthetic to match the RMS of an MHD synthetic which makes the full degradation non representative for the MHD case.

Finally, Fig. 2 shows the temperature stratification of two columns inverted from synthetics degraded with the ideal PSF but generated from an MHD atmosphere. As seen in the figure, despite one of the inverted columns being right on top of a magnetic bright point, the extracted temperature stratification matches surprisingly well with the known simulated atmosphere. Thus, despite the assumption of hydrostatic equilibrium, we can expect to extract the temperature stratification with accuracy even in small magnetic elements.

3. Temperature Gradients

In Fig. 3 two fields with magnetic features from the test observations were selected and compared with a random MHD snapshot. In

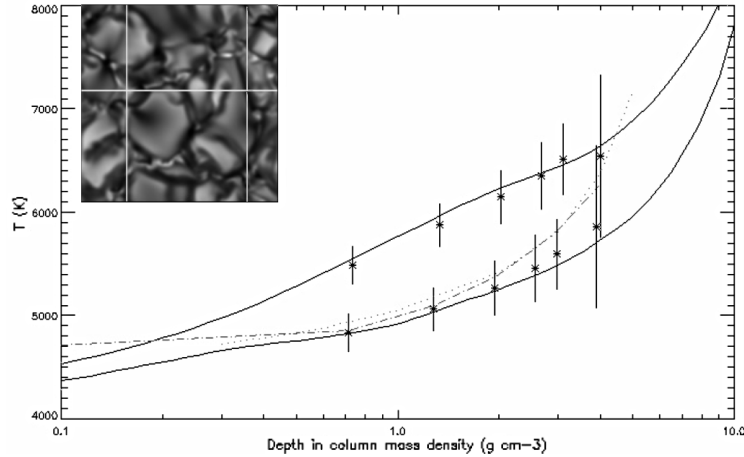


Fig. 2. The temperature stratification for two columns, inverted from degraded synthetic images, is shown. There are 6 points per inverted column corresponding to the 6 filter profiles in Fig.1 used to generate the synthetics. The solid lines are the respective known column stratifications from the 3D MHD simulated atmosphere. The horizontal position of the columns are signaled by the white crosshairs in the upper left image. The left crosshair marks the horizontal position of the column corresponding to the upper set of points while the right crosshair marks the bottom set. The plotted intervals are 3 times the $\sigma(T - T_{\text{real}})$. The dot-dashed line is the reference atmosphere used for calibration (dotted is the HoIMul atmosphere).

Table 1. Comparative statistics for extracted temperature and respective errors (values in kelvin).

	Observations	Ideal PSF	full degradation	Known HD Atmosphere
$\sigma(T)$	75	186	81	218
$\sigma(T - T_{\text{real}})$	–	97	111	–

the synthetic gradient map most transitions from a bright point to a granule follow the pattern: low gradient roughly centered in the intergranular lane, high gradient rim, low gradient rim, gradually increasing gradient up to the high gradient level of a granule. The same very fine pattern can be seen in the gradient maps derived from the observations. Higher concentration of bright points leads to a more direct transition of a low gradient area to the high gradient area of a granule in which case no rims are present in the observations and are either absent or diffuse in the synthetics. The presence of such fine features in both the synthetic images and the observations is intriguing, but further analysis is needed to guarantee that the observed features are not artifacts.

4. Conclusions

The tunable filter setup available at the SST's blue beam allows for extraction of the temperature stratification from the near continuum up to 300 km (where assumptions such as LTE begin to fail) in 0.1'' resolution and high cadence (one 3D map every 10 seconds). We tentatively see very fine features in the temperature gradients computed from observations of small magnetic elements which are also seen in synthetic images produced from MHD simulations. While observations like this are interesting in themselves, the greatest potential of this diagnostic resides in its future combination with full Stokes observations using the CRISP instrument at the SST's red beam.

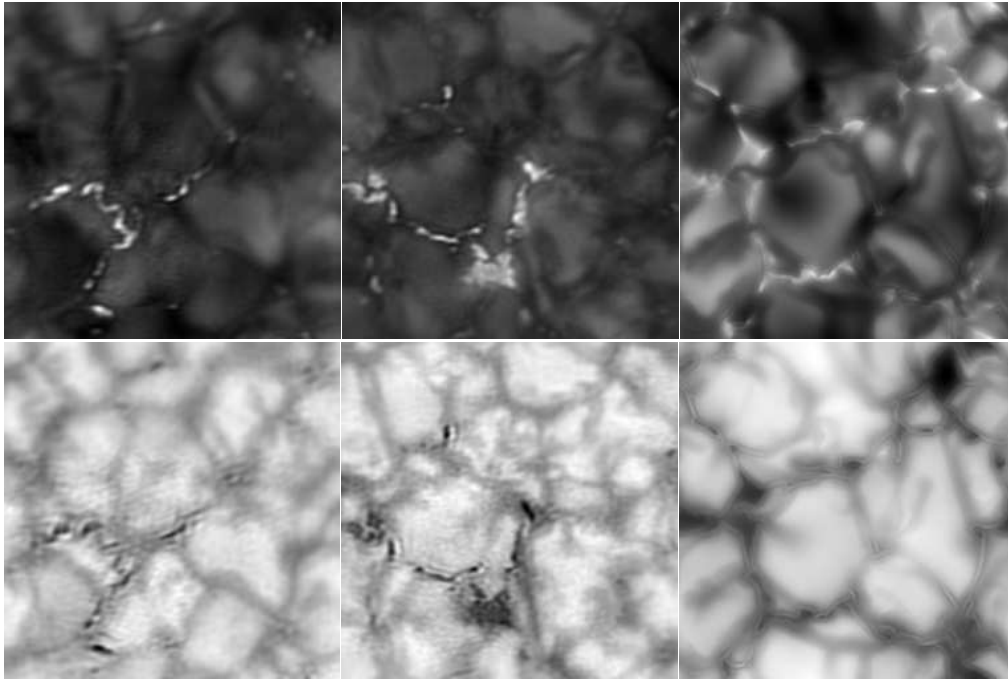


Fig. 3. Top left: Two different fields in intensity, average height of 2.97 g cm^{-3} (filter profile labeled as 4.7 in Fig. 1). Bottom left: dT/dm computed between the top position and the near continuum (profile labeled as 6.3 in Fig. 1 corresponding to an average height of 3.94 g cm^{-3}). Top right: degraded synthetic image from a MHD simulation snapshot generated using the same filter profiles as in top left. Bottom right: as in bottom left but for the synthetics obtained from the MHD simulation. $\mu = 1$ for all. Rims surrounding the intergranular lanes containing magnetic elements become apparent both in the synthetic and in the observation gradients (best seen at the bottom left quadrant of the central image).

Acknowledgements. We thank Mats Carlsson for making the simulation snapshots available, Jaime de La Cruz Rodriguez and Roald Schnerr for doing the observations and Mats Löfdahl for valuable input on the degradation scheme. This project is being supported by a Marie Curie Early Stage Research Training Fellowship of the European Communitys Sixth Framework Programme under contract number MEST-CT-2005-020395: The USO-SP International School for Solar Physics. The Swedish 1 m Solar Telescope is operated on La Palma by the Institute for Solar Physics of the Royal Swedish Academy of Sciences in the Spanish Observatorio del Roque de los Muchachos of the Instituto de Astrofísica de Canarias.

References

- Carlsson, M. 1986, Uppsala Astron. Obs. Report 33
- Holweger, H., & Mueller, E. A. 1974, *Sol. Phys.*, 39, 19
- Löfdahl, M. G., & Scharmer, G. 2004, *Solar Image Processing Workshop II*
- Piskunov, N. E., Kupka, F., Ryabchikova, T. A., Weiss, W. W., & Jeffery, C. S. 1995, *A&AS*, 112, 525
- Ryabchikova, T. A., Piskunov, N. E., Stempels, H. C., Kupka, F., & Weiss, W. W. 1999, *Physica Scripta Volume T*, 83, 162
- Shine, R. A., & Linsky, J. L. 1974, *Sol. Phys.*, 37, 145
- Stein, R. F., & Nordlund, A. 1998, *ApJ*, 499, 914
- van Noort, M., Rouppe van der Voort, L., & Löfdahl, M. G. 2005, *Sol. Phys.*, 228, 191
- Wedemeyer-Böhm, S., & Rouppe van der Voort, L. 2009, *A&A*, 503, 225